Author Manuscript

Author Manuscript

Author Manuscript

Author Manuscript

HHS Public Access

Author manuscript

Nucl Med Biol. Author manuscript; available in PMC 2019 September 01.

Published in final edited form as:

Nucl Med Biol. 2018 ; 64-65: 1–7. doi:10.1016/j.nucmedbio.2018.06.003.

Evaluation of a chloride-based ^{89}Zr isolation strategy using a tributyl phosphate (TBP)-functionalized extraction resin

Stephen A. Graves[a], **Christopher Kutyreff**[b], **Kendall E. Barrett**[b], **Reinier Hernandez**[c], **Paul A. Ellison**[b], **Steffen Happel**[d], **Eduardo Aluicio-Sarduy**[b], **Todd E. Barnhart**[b], **Robert J. Nickles**[b], and **Jonathan W. Engle**[b,*]

[a]Department of Radiation Oncology, University of Iowa, 200 Hawkins Dr., Iowa City, IA 52242, USA

[b]Department of Medical Physics, University of Wisconsin School of Medicine and Public Health, 1111 Highland Ave., Madison, WI 53705, USA

[c]Department of Radiology, University of Wisconsin School of Medicine and Public Health, 1111 Highland Ave., Madison, WI 53705, USA

[d]TrisKem International, 3 rue des champs Geons, 35170 Bruz, France

Abstract

Introduction: The remarkable stability of the ^{89}Zr-DOTA complex has been shown in recent literature. The formation of this complex appears to require ^{89}Zr-chloride as the complexation precursor rather than the more conventional ^{89}Zr-oxalate. In this work we present a method for the direct isolation of ^{89}Zr-chloride from irradiated ^{nat}Y foils.

Methods: ^{89}Zr, ^{88}Zr, and ^{88}Y were prepared by 16 MeV proton irradiation of ^{nat}Y foils and used for batch-extraction based equilibrium coefficient measurements for TBP and UTEVA resin. Radionuclidically pure ^{89}Zr was prepared by 14 MeV proton-irradiation of ^{nat}Y foils. These foils were dissolved in concentrated HCl, trapped on columns of TBP or UTEVA resin, and ^{89}Zr-chloride was eluted in < 1 mL of 0.1 M HCl. For purposes of comparison, conventionally-isolated ^{89}Zr-oxalate was converted to ^{89}Zr-chloride by trapping, rinsing, and elution from a QMA cartridge into 1 M HCl. Trace metal analysis was performed on the resulting ^{89}Zr products.

Results: Equilibrium coefficients for Y and Zr were similar between UTEVA and TBP resins across all HCl concentrations. K_d values of less than 10^{-1} mL/g were observed for Y across all HCl concentrations. K_d values of greater than 10^3 mL/g were observed at HCl concentrations greater than 9 M for Zr, falling to K_d values of less than 10° mL/g at low HCl concentrations. ^{89}Zr-chloride was recovered from small columns of TBP in <1 mL of 0.1 M HCl with an overall recovery efficiency of 89±3% (n=3). An average Y/Zr separation factor of 1.5×10^5 (n=3) was

*Corresponding author: Jonathan W. Engle; jwengle@wisc.edu; +1-608-263-5805.

Conflicts of Interest

TBP resin was provided at no cost for evaluation purposes by TrisKem International.

Publisher's Disclaimer: This is a PDF file of an unedited manuscript that has been accepted for publication. As a service to our customers we are providing this early version of the manuscript. The manuscript will undergo copyediting, typesetting, and review of the resulting proof before it is published in its final citable form. Please note that during the production process errors may be discovered which could affect the content, and all legal disclaimers that apply to the journal pertain.

Author Manuscript Author Manuscript Author Manuscript Author Manuscript

obtained. Trace metal impurities, notably Fe, were higher in TBP-isolated ^{89}Zr-chloride compared with ^{89}Zr-chloride prepared using the conventional two-step procedure.

Conclusion: TBP-functionalized resin appears promising for the direct isolation of ^{89}Zr-chloride from irradiated ^{nat}Y targets. Excellent ^{89}Zr recovery efficiencies were obtained, and chemical purity was sufficient for proof-of-concept chelation studies.

Keywords

immunoPET; positron emission tomography; zirconium-89; zr89

INTRODUCTION:

The use of ^{89}Zr ($t_{1/2}$: 3.27 d, β^+: 22.7%) in nuclear medicine has grown considerably in recent years, with more than 50 recruiting, active, or completed clinical trials in the United States. This adoption is due largely to developments in the field of immune-modulation therapy for a wide variety of solid and distributed cancers. The biological molecules and cells associated with immunotherapy typically exhibit slow tissue localization kinetics, with a blood-clearance half-life on the order of several days [1]. Positron emission tomography (PET) radiotracers are best designed when the pharmacokinetics of the compound are well-suited to the physical half-life of the radiolabel. The physical half-life of ^{89}Zr is therefore appropriate for the imaging of monoclonal antibodies several days post-injection. Another favorable aspect of ^{89}Zr is that it may be produced in large quantities on a low energy medical cyclotron by proton irradiation of naturally monoisotopic yttrium metal. Recent work has shown that more than 40 patient doses worth of radioactivity (~185 MBq / 5 mCi per administration) may be produced in a four hour irradiation [2]. This availability combined with a half-life conducive to international transport has led to ^{89}Zr being the most commonly used radioisotope in immune system-related nuclear medicine studies.

Isolation of ^{89}Zr from proton irradiated ^{nat}Y targets has conventionally been achieved through trapping from a hydrogen chloride solution onto hydroxamate-functionalized resins, followed by elution with oxalic acid [3–5]. This method has proven robust for radiochemical isolation and may result in apparent molar activities - as measured by titration with desferoxamine (DFO) - of greater than 37 GBq/μmol (1 Ci/μmol) regularly [2]. Unfortunately, significant instability is observed with ^{89}Zr-DFO-based bioconjugates *in vivo* [6–8]. ^{89}Zr dissociation on the order of 5 – 10% at 48 hours postinjection is commonly observed in a murine model with the unbound ^{89}Zr accumulating in radiosensitive bone. This chelation instability may significantly impact the usefulness of some radiotracers, particularly where quantitation is used to monitor the progression of disease or in the case of external-beam radiotherapy target delineation. Off-target bone uptake may also decrease the diagnostic utility of tracers that could otherwise reveal lesions proximal to bone, such as metastatic prostate cancer.

Significant efforts have been made to produce new chelators or derivatives of DFO that offer improved *in vivo* ^{89}Zr complexation stability [9–19]. Recent work has also shown remarkable stability of the ^{89}Zr-DOTA complex [8]. Unfortunately, formation of the ^{89}Zr-DOTA complex appears to require ^{89}Zr to be in the form of ^{89}Zr-chloride rather than ^{89}Zr-

Author Manuscript Author Manuscript Author Manuscript Author Manuscript

oxalate prior to chelation. The ^{89}Zr-oxalate resulting from the conventional hydroxamate-based separation may be reconstituted as ^{89}Zr-chloride by trapping on an activated quaternary methyl ammonium (QMA) anion exchange cartridge, followed by rinsing, followed by elution in ~500 μL of 1 M HCl [3, 20, 21]. Although this method appears effective for reconstitution as ^{89}Zr-chloride, a direct chloride-based ^{89}Zr/^{nat}Y separation strategy would be preferred; such a separation would offer the complete absence of the oxalate anion (<0.2% residual oxalate measured in QMA-prepared ^{89}Zr-chloride by Holland et al. [3]) and might offer simplified radiochemistry automation and improved overall ^{89}Zr recovery.

The purpose of this work was to devise a column-based Y/Zr radiochemical separation method with elution in a small volume of weak HCl. Based on a favorable difference in the equilibrium coefficients for Zr and Y in mixtures of tributyl phosphate (TBP) and HCl [22], an experiment was designed to measure the HCl-based equilibrium coefficients of Zr and Y for the solid-phase extraction resin UTEVA (Eichrom Technologies LLC) and for a TBP-impregnated solid-phase resin (TrisKem International). Following the measurement of these equilibrium coefficients, an HCl-based Zr/Y separation strategy was proposed and tested. As the resulting chemical purity is essential to the usefulness of such a technique, this new ^{89}Zr-chloride product was compared against conventionally isolated ^{89}Zr-oxalate and ^{89}Zr-chloride via trace metal analysis. Chelation experiments were also performed to demonstrate the reactivity of the ^{89}Zr-chloride resulting from TBP-based isolation.

MATERIALS AND METHODS:

General experimental details

Any reference to “^{89}Zr-chloride” refers to the equilibrium mixture of free ^{89}Zr cations, chloride-speciations, and aquated forms of ^{89}Zr. “^{89}Zr-chloride” isolated from oxalate-based solutions using a QMA cartridge does contain residual oxalate anion. In this case, although we refer to this product as “^{89}Zr-chloride,” it is likely that the majority of ^{89}Zr remains coordinated with oxalate anions. The choice to refer to this product as “^{89}Zr-chloride” stems from the fact that this product does indeed show chelation by DOTA, while chelation from the original oxalate solution does not appear tractable.

Unless otherwise stated, all chemicals were obtained from Sigma Aldrich. UTEVA resin was purchased from Eichrom Technologies LLC (Lisle, IL 60532, USA). The TBP-impregnated resin (herein referred to as ‘TBP resin’) was provided at no cost by TrisKem International (Bruz, France) for evaluation purposes. Hydrochloric acid (aq. HCl 35–38%; Optima Grade, Fisher Scientific) was titrated and found to have a concentration of 10.96 ± 0.11 M. Any reference herein to “concentrated HCl” refers to this solution. All other concentrations of HCl used were prepared from this batch by dilution with >18 MΩ/cm H_2O. ^{89}Zr sample activities in excess of 1 MBq were quantified by dose calibrator (Capintec CRC-15r) assay using calibration number 489. All other sample activities were quantified by efficiency-calibrated high-purity germanium gamma spectrometry.

Column masses are specified as dry resin, weighed by mass-balance. Columns were prepared by placing a 20 μm porosity frit at the bottom of a 1 mL column (polypropylene,

Author Manuscript Author Manuscript Author Manuscript Author Manuscript

5.6 mm ID). Resin was added, and a 20 μm top-frit was placed above the resin. Columns were rinsed with >10 column volumes of 0.1 M HCl and concentrated HCl prior to equilibration for all experiments.

Apparent molar activity (formerly effective specific activity) is defined as the activity of a sample divided by twice the quantity of chelate required to obtain 50% binding.

Unless otherwise specified, all values ($x \pm \sigma$) represent mean ± standard deviation.

Gamma Spectroscopy

A high-purity germanium (HPGe, Canberra C1519) gamma detector was calibrated for efficiency and energy response using point sources of ^{60}Co, ^{137}Cs, ^{133}Ba, and ^{241}Am obtained from the National Institute of Standards and Technology (NIST) and an in-house quantified point-source of ^{152}Eu. Gamma spectrum peak areas were determined using the SAMPO algorithm [23] within the FitzPeaks software platform. Second-order Bateman calculations were used for decay correction of the ^{88}Y/^{88}Zr pair during experimentation.

Preparation of Radioactivity

For equilibrium coefficient experiments, a ^{nat}Y foil (99.5%, 400 mg, Alfa Aesar) was irradiated by 16 MeV with a beam current of 10 μA for one hour. The resulting foil was allowed to decay for two weeks. Following this period of decay, the abundances of ^{88}Y ($t_{1/2}$: 106.6 d), ^{88}Zr ($t_{1/2}$: 83.4 d), and ^{89}Zr were quantified by efficiency-calibrated high-purity germanium (HPGe) gamma spectroscopy. This foil was dissolved in 3 mL of concentrated HCl, added drop-wise at room temperature in open atmosphere.

For radiochemical isolation experiments, a ^{nat}Y target (99.5%, 400 mg, Alfa Aesar) was prepared as previously described by resistive spot-welding onto a tantalum target backing [2]. These targets were irradiated by 50 μA of beam current, degraded to an average energy 14 MeV by a 0.125 mm Mo foil to limit the production of ^{88}Y/^{88}Zr. These targets were dissolved from the tantalum backing by 10 mL of concentrated HCl, added drop-wise at room temperature in open atmosphere.

Equilibrium Coefficient Measurements

Aliquots of radioactivity (40 μL, ~370 kBq/10 μCi ^{89}Zr, ~37 kBq/1 μCi ^{88}Y) were added to 1.5 mL centrifuge vials containing 1000 μL of HCl (0 M, 1 M, 3 M, 5 M, 7 M, 9 M, or 10.96 M) and approximately 110 mg of dry resin (UTEVA or TBP; measured by mass balance difference and recorded for each sample). Uncertainty in acid concentration was determined from uncertainty in the pipetted volume of radioactivity added in quadrature with uncertainty in the stock HCl concentration. A final HCl concentration for each sample following the addition of radioactivity was calculated based on residual acidity in the dissolved target solution. Residual acidity was calculated by assuming that four protons were consumed per atom of dissolved Zr. Samples were placed on a multi-vial vortexer (Fisher Scientific) at room temperature for 24 hours at maximum speed. The mixture from each sample was then passed over a small fritted-column by pipette transfer in order to isolate the majority of the liquid phase in a new vial. The mass of this collected liquid phase

Author Manuscript Author Manuscript Author Manuscript Author Manuscript

was determined by subtractive weighing. Columns containing filtered resin were placed within their respective original centrifuge vial for further spectroscopic analysis. The solid and liquid phases of each sample were analyzed by HPGe gamma spectroscopy to determine the distribution of ^{88}Y, ^{88}Zr, and ^{89}Zr between phases.

Equilibrium coefficients were calculated as the amount of radioactivity bound to the resin per mass of dry resin, divided by the amount of radioactivity in solution per mass of solution. A linear relationship between the density and molarity of HCl was assumed, with 10.96 M HCl having density 1.172 g/mL and water having a density of 1.000 g/mL. Uncertainty in measured equilibrium coefficients included uncertainty in radioactivity quantification, uncertainty in decay corrections, and uncertainty in the fraction of isolated liquid phase - added in quadrature. As the ^{88}Zr and ^{89}Zr elemental tracers provide complimentary information, the equilibrium coefficients for Zr presented herein represent the average of these data.

Binding Kinetics Evaluation

To determine the rate at which equilibrium is approached during mixing, samples were created containing 1000 μL of concentrated HCl and approximately 110 mg of dry resin (UTEVA or TBP; measured for each sample by mass balance difference). To these samples, 40 μL of radioactivity was added, as with equilibrium coefficient measurements. Samples were placed on a multi-vial vortexer, and one sample for each resin type was removed at serial time-points (10 s, 60 s, 1 min, 5 min, 30 min, and 3 h). Immediately after removing a sample from the vortex apparatus, the mixture was passed over a small fritted-column by pipette transfer in order to isolate the majority of the liquid phase in a new vial. 600 μL of this liquid phase was isolated for analysis by HPGe gamma spectroscopy. The fraction of ^{88}Y, ^{88}Zr, and ^{89}Zr contained within the liquid fraction was determined by dividing the measured radioactivity by the fraction of liquid volume used for counting. The residual amount of radioactivity on the resin at the point of vortex cessation was calculated as the residual, relative the activity in the liquid phase. As with equilibrium coefficient measurements, the results from ^{88}Zr and ^{89}Zr were averaged for kinetics determination.

Column Chromatography Method Development

To determine optimal separation conditions, a series of experiments were performed. First, column loading speed was evaluated by passing ~1.9 MBq (50 μCi) of ^{89}Zr and ~70 mg ^{nat}Y in 5 mL of 9.6 M HCl over 100 mg columns of TBP and UTEVA resins at 1 mL/min and 5 mL/min. Columns were subsequently rinsed with 5 mL of 9.6 M HCl and ^{89}Zr trapping efficiency was measured by dose calibrator survey of the column and pass-through. Next, four columns were prepared - two containing 100 mg of UTEVA resin and two containing 100 mg of TBP resin. Approximately 1.9 MBq (50 μCi) of ^{89}Zr was trapped onto each column from a solution of 9.6 M HCl. Elution of radioactivity from columns was performed using 1 mL of 0.1 M HCl or 1 mL of 3 M HCl for each resin type. Elution efficiency was quantified by dose calibrator survey of the eluent from each column. Finally, elution profiles were measured from columns containing 100 mg UTEVA resin or TBP resin that had been loaded with ~3.8 MBq (100 μCi) of ^{89}Zr in 9.6 M HCl and rinsed with 5 mL of 9.6 M HCl. Elution was performed with ~2 mL of 0.1 M HCl, collecting eluent in a series of 1.5 mL

Author Manuscript Author Manuscript Author Manuscript Author Manuscript

microcentrifuge tubes. The mass of eluent collected in each vial was determined by subtractive weighing, and the radioactivity in each vial was measured by dose calibrator survey.

Zr/Y Radiochemical Separation

Due to the superior elution properties observed herein, TBP resin was selected for full-scale Zr/Y separation experiments. A column containing TBP resin (220 mg, 5.6 mm inner diameter) was prepared by rinsing with 10 mL of 0.1 M HCl, followed by rinsing with 10 mL of 3 M HCl, followed by equilibration with 10 mL of 9.6 M HCl. A 10 mL dissolved target solution containing ^{89}Zr and ~400 mg ^{nat}Y in ~9.6 M HCl was loaded onto this column at approximately 2 mL/min. The column was then rinsed with 20 mL of 9.6 M HCl and eluted with 1 mL of 0.1 M HCl flowing at 0.5 mL/min. This separation procedure was conducted three times to evaluate method robustness.

For comparative purposes, ^{89}Zr-oxalate was produced by conventional means (n = 3) [2, 3]. Briefly, commercially available hydroxamate-functionalized extraction chromatography resin (Zr resin, TRISKEM, 500–100 μm) was equilibrated with 10 mL of water and 10 mL of 2 M HCl. The ^{nat}Y foil was dissolved in 5 mL of 6 M HCl, diluted with the addition of 10 mL water and loaded onto the equilibrated Zr resin column (100 mg, 5.6 mm inner diameter). This column was subsequently rinsed with 10 mL of 2 M HCl and 10 mL of H_2O, and ^{89}Zr-oxalate was eluted in approximately 500 μL of 1 M oxalic acid. An aliquot of this ^{89}Zr-oxalate for each production was converted to ^{89}Zr-chloride by previously published methods [3, 20, 21]. Briefly a Sep-Pak Accell Light QMA cartridge (Waters Corp.) was prepared by rinsing with 6 mL of MeCN and 20 mL of H_2O. ^{89}Zr in 1 M oxalic acid was quantitatively loaded onto this QMA cartridge. The cartridge was rinsed by >40 mL of H_2O to remove residual oxalate anion, and the activity was eluted in 1 mL of 1 M HCl with greater than 90% efficiency.

Trace metal analysis

Residual ^{nat}Y in the isolated ^{89}Zr-chloride and ^{89}Zr-oxalate products was quantified by microwave plasma atomic emission spectrometry (MP-AES, Agilent 4200). Separation factors were calculated for each of the production runs based on residual ^{nat}Y and recovery efficiency of ^{89}Zr. In addition to ^{nat}Y, trace quantities of Zr, Ni, Fe, Mo, Cr, Mn, Zn, Co, and Cu were also measured by MP-AES to evaluate residual target impurities in the separated ^{89}Zr products. For purposes of comparison between production methods, trace metal burdens were normalized to values that would be expected from a full-target production run.

DOTA andDFO Chelation of ^{89}Zr

^{89}Zr-chloride apparent molar activity was measured by DOTA titration as follows: vials were prepared containing increasing quantities of DOTA (100 μL of 0, 1, 3, 10, 30, 100, 300 μg/mL in H_2O). To each of these vials, 0.5 M HEPES buffer (100 μL, pH 7.5) and NaOH were added (50 μL, 0.1 M or 1.0 M). ^{89}Zr-chloride (50 μL, 0.1 M or 1.0 M HCl) was added to each vial for a total volume of 300 μL and a final pH of ~7.0. Solutions were allowed to react at 90 °C for 45 minutes. Thin layer chromatographs were run (Al-backed silica gel 50 F_{254}, MilliporeSigma Inc., 1:1 MeOH : 10% NH4OAc w/v mobile phase) to separate

Author Manuscript Author Manuscript Author Manuscript Author Manuscript

bound and unbound ^{89}Zr. Under this chromatography system, unbound ^{89}Zr remains at the origin with a retention factor of zero (R_f=0), while ^{89}Zr-DOTA travels with the mobile-phase (R_f~0.3). Activity distribution on the TLC plate was measured by autoradiography (Cyclone, Perkin Elmer Inc.).

^{89}Zr-oxalate effective molar activity by DFO chelation was measured as follows: ^{89}Zr-oxalate (60 μL, 1 M oxalic acid) was added to HEPES buffer (1.2 mL, 0.25 M, pH 10) yielding a final solution of pH 8. Vials were prepared containing increasing quantities of DFO (100 μL of 0, 0.1, 0.3, 1, 3, 10, 30 μg/mL in H_2O), and to each of these vials 100 μL of buffered activity was added. Solutions were allowed to react at room temperature for one hour. Following this reaction time, an excess of DTPA (400 μL, 0.05 M) was added to conjugate residual free ^{89}Zr. Thin layer chromatographs were run (Al-backed silica gel 50 F_{254}, MilliporeSigma Inc., 0.05 M DTPA mobile phase) in order to separate ^{89}Zr-DFO and ^{89}Zr- DTPA. Under this chromatography system, ^{89}Zr-DFO remains at the origin (R_f=0), while ^{89}Zr-DTPA travels with the mobile phase (R_f=0.7). Activity distribution on the TLC plate was measured by autoradiography (Cyclone, Perkin Elmer Inc.).

RESULTS:

Equilibrium coefficients

In HCl concentrations greater than 5 M both the UTEVA and TBP resins floated at the top of each sample vial, even with repeated centrifuging. This prevented the assay from being conducted by pelleting the resin material and drawing aliquots from the samples' supernatant. Isolating the liquid phase by filtration was effective, but introduced the possibility of radioisotope sorption onto the column frit. To test this possibility, a sample of ^{88}Y, ^{88}Zr, and ^{89}Zr in concentrated HCl was passed over a small column, without the presence of resin. No loss in radioactivity was observed through this process, suggesting that the filtration method was appropriate. The resins' buoyancy suggests the use of a 'top-frit' in column- based experiments.

A complete set of measured equilibrium coefficients for Y and Zr on the UTEVA and TBP-impregnated resins are listed in Supplementary Table 1. These measured equilibrium coefficients are plotted as a function of HCl concentration and resin type in Figure 1, alongside literature values for TBP solvent-solvent extraction equilibrium coefficients for Zr [22]. The equilibrium coefficients measured herein generally agree with expected TBP-solvent values, except at low HCl concentrations where both UTEVA and TBP resins retained more Zr. A maximum equilibrium coefficient of ~5×10^3 mL/g observed at HCl concentrations of 9 M or higher for both resins. This suggests that either resin is appropriate for trapping $^{89}Zr^{4+}$ at these acid concentrations, and that the radioactivity may be readily eluted with HCl concentrations below 6 M. ^{88}Y was not retained strongly by either resin at any HCl concentration, having measured equilibrium coefficients less than 1×10^{-1} mL/g at all acid concentrations.

Author Manuscript Author Manuscript Author Manuscript Author Manuscript

Binding Kinetics

^{89}Zr sorption onto TBP and UTEVA resin as a function of time from solutions of 10.96 ± 0.11 M HCl is shown in Figure 2A. Significantly faster kinetics are observed with the TBP resin compared with the UTEVA resin despite comparable equilibrium coefficients at these acid concentrations. TBP sorption of ^{89}Zr exceeded 95% within 30 seconds, while UTEVA resin took approximately 5 minutes to reach this point.

Column Chromatography Method Development

A high degree of ^{89}Zr retention (>85%) was observed for both UTEVA and TBP columns (~100 mg) when loading with low burdens of ^{nat}Y (<100 mg). Trapping efficiencies were somewhat sensitive to loading flow rate, as shown in Figure 2B. Trapping on UTEVA saw a greater trapping efficiency improvement (~3.5%) when loading 1 mL/min rather than 5 mL/min, compared with TBP resin which saw only a ~2% efficiency gain. This is consistent with results from binding kinetics measurements for the TBP and UTEVA resins, although the difference is marginal in practice.

Elution of ^{89}Zr from both UTEVA and TBP was rapid and complete when using 3 M HCl, however eluting in 0.1 M HCl resulted in incomplete elution from UTEVA resin. The ~29% residual activity on UTEVA columns after initial 0.1 M HCl washes could be readily removed by increasing the HCl concentration to 3 M. This behavior is in disagreement with the equilibrium coefficients for Zr on UTEVA measured herein, assuming Zr/UTEVA behaves similarly in 0.1 M and 0.26 M HCl. An elution profile of ^{89}Zr-chloride from 100 mg columns of UTEVA and TBP using 0.1 M HCl is shown in Figure 3. Although UTEVA retained a significant fraction of ^{89}Zr, the two columns had very similar elution profiles, with the majority of activity being eluted in the first 500 μL of 0.1 M HCl.

TBP-basedRadiochemical Separation Results

An average ^{89}Zr-chloride recovery efficiency of 89 ± 3% (n = 3) was obtained with the TBP-based separation method described herein. Approximately one third of unrecovered activity was lost at each separation step: loading, rinsing, and elution. Eluent was typically pale yellow in color, however trace metal analysis revealed an average residual ^{nat}Y mass of 4.3 ± 4.5 μg (n = 3). These measurements, combined with the fact that YCl_3 is colorless in solution, seems to suggest that the pale yellow color was due to formation of dissolved Cl_2 gas rather than trace metal impurities. It is also possible that the color was due to the presence of trace divalent iron. Concurrent with loading of the target solution, the resin turned a pale grey color, and the top and bottom column frits turned a dark gray color. This color remained unchanged during rinsing and elution. An average separation factor of (1.5 ± 1.0) x10^5 (n = 3) was measured, which corresponds to physical molar activities of 18 −104 GBq/μmol (0.5 – 2.8 Ci/μmol) Y for a typical 1.85 GBq (50 mCi) production. Separation details from individual ^{89}Zr production runs are listed in Table 1.

The quantity of residual ^{nat}Y in the eluted product was found to depend strongly on the volume of 9.6 M rinse following ^{89}Zr trapping. Three production runs were performed with only a 5 mL 9.6 M HCl rinse prior to elution. In these experiments, an average residual ^{nat}Y mass of 35 ± 16 μg (n = 3) was observed, significantly higher than the mass reported above

Author Manuscript Author Manuscript Author Manuscript Author Manuscript

following a 20 mL rinse. It is possible that residual ^{nat}Y could be further reduced by additional rinsing, but at the cost of reduced ^{89}Zr recovery.

Trace Metal Analysis Comparison

Quantities of trace metal impurities in the TBP-based isolated ^{89}Zr-chloride are shown in Figure 4 and tabulated in Supplementary Table 2. Although increased rinsing was shown to significantly reduce Y mass in the final product, the mass of Fe was found to be unaffected by changes in rinsing, with 32.7 ± 3.4 μg observed for separations employing 5 mL rinse steps (n = 3) and 38.8 ± 3.4 μg in separations employing 20 mL rinse steps (n = 3). The abundance of Mo as a trace metal impurity is ostensibly due to sputtering from the Mo degrader foil used approximately 2.5 mm above the ^{nat}Y target surface during irradiation, although it is also possible that Mo impurities exist within the target material.

DOTA and DFO Chelation of ^{89}Zr

Example chromatographs of ^{89}Zr-DFO and ^{89}Zr-DOTA chelation are shown in Figure 5. ^{89}Zr-DOTA formation was successfully observed under the following conditions: temperatures greater than 60 °C; pH 5.0–7.5; and DOTA concentrations greater than 4 μg/mL. Chelation was found to be most efficient (>90% yield) at pH 7.0, temperatures above 90 °C, and DOTA concentrations greater than 40 μg/mL. Hydrolysis was a significant effect, as evidenced by drastic differences in the measured apparent molar activity between the two preparations of ^{89}Zr-chloride. Specifically, the average apparent molar activity for TBP-separated ^{89}Zr-chloride was measured to be 85 ± 48 MBq/μmol (2.3 ± 1.1 mCi/μmol, n = 3) while QMA-reconstituted ^{89}Zr-chloride had a measured effective molar activity of 518 ± 56 MBq/μREmol (14.0 ± 1.5 mCi/μmol, n = 3). It is not clear whether this discrepancy in DOTA apparent molar activity is as a result of differences in the method of ^{89}Zr-chloride activity preparation (TBP-isolated vs QMA-reconstituted), labeling ionic strength (0.017 M vs 0.17 M, respectively), or labeling radioactivity concentration (~2.5 MBq/mL vs ~12.2 MBq/mL, respectively). ^{89}Zr-oxalate apparent molar activity - as measured by DFO chelation - was found to be significantly higher with a measured average of 75 ± 8 GBq/μmol (2030 ± 230 mCi/μmol, n = 3). This average is consistent with the historic average of 59 ± 48 GBq/μmol (1600 ± 1300 mCi/μmol, n = 124) at the University of Wisconsin [2].

DISCUSSION:

The stable chelation of ^{89}Zr is an area of significant focus in preclinical nuclear medicine, with several institutions working to offer tractable solutions [9–14, 16, 18, 19]. One approach appears to be conjugation of ^{89}Zr from its chloride salt by the widely-used DOTA chelator. In a chelation challenge study, Pandya et al. found that ^{89}Zr-DOTA remains 100% stable after incubation for 7 days at 37 °C, pH 7.0 with a 1000-fold excess competing EDTA, while ^{89}Zr-DFO fell to 20.3% stability under identical conditions [8]. The remarkable stability of the ^{89}Zr-DOTA complex and efficient formation thereof recently described by Pandya et al. has led our group to investigate alternate production pathways for ^{89}Zr-chloride that do not include use of the oxalate anion.

Author Manuscript Author Manuscript Author Manuscript Author Manuscript

Solutions of tributyl phosphate (TBP) in kerosene are commonly used for extraction of uranium, thorium, and plutonium from spent nuclear fuel rods which have been dissolved in nitric acid. This application has likely been a major motivation in the development of solid-phase TBP-like extraction resins [24–26]. These developments have presented an opportunity in radiopharmaceutical applications for innovative separation strategies, as evidenced by the recent growth in radiochemistry literature employing solid-phase extraction resins [27–29]. Two such resins include the TBP-impregnated resin and the Uranium and Tetravalent Actinides extraction resin (UTEVA, Eichrom Technologies LLC) dipentyl pentylphosphonate- (DAAP-) functionalized extraction resin. The structures for these extractants are shown in Figure 6. Published TBP equilibrium coefficients for Zr and Y indicate strong sorption of Zr from HCl-based solutions with little affinity for Y [22]. Due to the similar molecular structure of DAAP and TBP, we hypothesized that UTEVA resin could also be used to isolate Zr from Y, in spite of there being no published data to this effect.

An additional drawback of the ^{89}Zr-DOTA chelation reaction is the high reaction temperature; Pandya et al. described chelation at 95 °C, and this temperature was qualitatively found to be appropriate within our own work. Chelation at lower temperatures appears to drastically reduce DOTA complexation kinetics, allowing for substantial relative increases in hydrolysis. Most large biological molecules, such as monoclonal antibodies, are incapable of tolerating such elevated temperatures. The use of the ^{89}Zr-DOTA complex in nuclear medicine will likely depend on pre-chelation followed by bioconjugation, such as the methods used by Bansal ***et al.*** [31] or Zeglis ***et al.*** [32].

CONCLUSION:

The use of a TBP-functionalized resin for the direct isolation of ^{89}Zr-chloride from irradiated ^{nat}Y targets appears promising. Excellent ^{89}Zr recovery efficiencies were obtained, and chemical purity was sufficiently high for proof-of- concept chelation studies. This work may enable further developments in the pursuit of high-stability ^{89}Zr-containing compounds. Further work is needed to address hydrolysis and the requisite elevated temperatures during ^{89}Zr-DOTA complexation in the context of bioconjugate applications.

Supplementary Material

Refer to Web version on PubMed Central for supplementary material.

Acknowledgements

We gratefully acknowledge support from the University of Wisconsin - Madison and the National Institutes of Health (T32-CA009206).

References

[1]. Deri MA, Zeglis BM, Francesconi LC, and Lewis JS. PET imaging with ^{89}Zr: from radiochemistry to the clinic. Nuclear medicine and biology 2013;40:3–14. [PubMed: 22998840]

[2]. Ellison PA, Valdovinos HF, Graves SA, Barnhart TE, and Nickles RJ. Spot-welding solid targets for high current cyclotron irradiation. Applied Radiation and Isotopes 2016;118:350–3. [PubMed: 27771445]

Author Manuscript Author Manuscript Author Manuscript Author Manuscript

[3]. Holland JP, Sheh Y, and Lewis JS. Standardized methods for the production of high specific-activity zirconium-89. Nuclear medicine and biology 2009;36:729–39. [PubMed: 19720285]

[4]. Verel I, Visser GW, Boellaard R, Stigter-van Walsum M, Snow GB, and van Dongen GA. ^{89}Zr immuno-PET: comprehensive procedures for the production of ^{89}Zr-labeled monoclonal antibodies. Journal of nuclear medicine 2003;44:1271–81. [PubMed: 12902418]

[5]. Wooten A, Madrid E, Schweitzer GD, Lawrence LA, Mebrahtu E, Lewis BC, et al. Routine production of ^{89}Zr using an automated module. Applied Sciences 2013;3:593–613.

[6]. Holland JP, Divilov V, Bander NH, Smith-Jones PM, Larson SM, and Lewis JS. ^{89}Zr-DFO-J591 for immunoPET of prostate-specific membrane antigen expression in vivo. Journal of Nuclear Medicine 2010;51:1293–300. [PubMed: 20660376]

[7]. Abou DS, Ku T, and Smith-Jones PM. In vivo biodistribution and accumulation of 89 Zr in mice. Nuclear medicine and biology 2011;38:675–81. [PubMed: 21718943]

[8]. Pandya DN, Bhatt N, Yuan H, Day CS, Ehrmann BM, Wright M, et al. Zirconium tetraazamacrocycle complexes display extraordinary stability and provide a new strategy for zirconium-89-based radiopharmaceutical development. Chemical Science 2017;8:2309–14. [PubMed: 28451334]

[9]. Vugts DJ, Klaver C, Sewing C, Poot AJ, Adamzek K, Huegli S, et al. Comparison of the octadentate bifunctional chelator DFO*-pPhe-NCS and the clinically used hexadentate bifunctional chelator DFO-pPhe-NCS for ^{89}Zr-immuno- PET. European journal of nuclear medicine and molecular imaging 2017;44:286–95. [PubMed: 27573793]

[10]. Deri MA, Ponnala S, Kozlowski P, Burton-Pye BP, Cicek HT, Hu C, et al. p-SCN-Bn-HOPO: A superior bifunctional chelator for ^{89}Zr immunoPET. Bioconjugate chemistry 2015;26:2579–91. [PubMed: 26550847]

[11]. Patra M, Bauman A, Mari C, Fischer CA, Blacque O, Haussinger D, et al. An octadentate bifunctional chelating agent for the development of stable zirconium-89 based molecular imaging probes. Chemical Communications 2014;50:11523–5. [PubMed: 25132321]

[12]. Deri MA, Ponnala S, Zeglis BM, Pohl G, Dannenberg J, Lewis JS, et al. Alternative chelator for ^{89}Zr radiopharmaceuticals: radiolabeling and evaluation of 3, 4, 3-(LI-1, 2-HOPO). Journal of medicinal chemistry 2014;57:4849–60. [PubMed: 24814511]

[13]. Guerard F, Lee YS, and Brechbiel MW. Rational design, synthesis, and evaluation of tetrahydroxamic acid chelators for stable complexation of zirconium (IV). Chemistry-A European Journal 2014;20:5584–91.

[14]. Guerard F, Lee Y-S, Tripier R, Szajek LP, Deschamps JR, and Brechbiel MW. Investigation of Zr (IV) and ^{89}Zr (IV) complexation with hydroxamates: progress towards designing a better chelator than desferrioxamine B for immuno- PET imaging. Chemical Communications 2013;49:1002–4. [PubMed: 23250287]

[15]. Holland JP and Vasdev N. Charting the mechanism and reactivity of zirconium oxalate with hydroxamate ligands using density functional theory: implications in new chelate design. Dalton Transactions 2014;43:9872–84. [PubMed: 24722728]

[16]. Ma MT, Meszaros LK, Paterson BM, Berry DJ, Cooper MS, Ma Y, et al. Tripodal tris (hydroxypyridinone) ligands for immunoconjugate PET imaging with $^{89}Zr^{4+}$: comparison with desferrioxamine-B. Dalton Transactions 2015;44:4884–900. [PubMed: 25351250]

[17]. Pandya DN, Pailloux S, Tatum D, Magda D, and Wadas TJ. Di-macrocyclic terephthalamide ligands as chelators for the PET radionuclide zirconium-89. Chemical Communications 2015;51:2301–3. [PubMed: 25556851]

[18]. Zhai C, Summer D, Rangger C, Franssen GM, Laverman P, Haas H, et al. Novel bifunctional cyclic chelator for ^{89}Zr labeling-radiolabeling and targeting properties of RGD conjugates. Molecular pharmaceutics 2015;12:2142–50. [PubMed: 25941834]

[19]. Adams CJ, Wilson JJ, and Boros E. Multifunctional Desferrichrome Analogues as Versatile ^{89}Zr (IV) Chelators for ImmunoPET Probe Development. Molecular pharmaceutics 2017;14:2831–42. [PubMed: 28665620]

[20]. Sato N, Wu H, Asiedu KO, Szajek LP, Griffiths GL, and Choyke PL. ^{89}Zr-oxine complex PET cell imaging in monitoring cell-based therapies. Radiology 2015;275:490–500. [PubMed: 25706654]

Author Manuscript Author Manuscript Author Manuscript Author Manuscript

[21]. Lin M, Mukhopadhyay U, Waligorski GJ, Balatoni JA, and Gonzalez-Lepera C. Semi-automated production of ^{89}Zr- oxalate/^{89}Zr-chloride and the potential of ^{89}Zr-chloride in radiopharmaceutical compounding. Applied Radiation and Isotopes 2016;107:317–22. [PubMed: 26595775]

[22]. Braun T and Ghersini G. Extraction chromatography: Elsevier,1975.

[23]. Aarnio P, Nikkinen M, and Routti J. SAMPO 90 High resolution interactive gamma-spectrum analysis including automation with macros. Journal of radioanalytical and nuclear chemistry 1992;160:289–95.

[24]. Warshawsky A and Patchomik A. Impregnated Resins: Metal-Ion Complexing Agents Incorporated Physically In Polymeric Matrices. Israel Journal of Chemistry 1978;17:307–15.

[25]. Serrano J and Kimura T. Extraction chromatography in the TBP-HNO3 system. Journal of radioanalytical and nuclear chemistry 1993;172:97–105.

[26]. Pilvio R and Bickel M. Actinide separations using extraction chromatography. Environmental Changes and Radioactive Tracers 2002:139–48.

[27]. Valdovinos HF, Graves S, Barnhart T, and Nickles RJ. Simplified and reproducible radiochemical separations for the production of high specific activity ^{61}Cu, ^{64}Cu, ^{86}Y and ^{55}Co. AIP Conference Proceedings: AIP Publishing; 2017, p. 020021.

[28]. Rodriguez R, Avivar J, Leal LO, Cerda V, and Ferrer L. Strategies for automating solid-phase extraction and liquidliquid extraction in radiochemical analysis. TrAC Trends in Analytical Chemistry 2016;76:145–52.

[29]. Müller C, Bunka M, Haller S, Köster U, Groehn V, Bernhardt P, et al. Promising prospects for ^{44}Sc-/^{47}Sc-based theragnostics: application of ^{47}Sc for radionuclide tumor therapy in mice. Journal of nuclear medicine 2014;55:1658–64. [PubMed: 25034091]

[30]. Hennig C, Weiss S, Kraus W, Kretzschmar J, and Scheinost AC. Solution species and crystal structure of Zr (IV) acetate. Inorganic chemistry 2017;56:2473–80. [PubMed: 28199091]

[31]. Bansal A, Pandey MK, Demirhan YE, Nesbitt JJ, Crespo-Diaz RJ, Terzic A, et al. Novel ^{89}Zr cell labeling approach for PET-based cell trafficking studies. EJNMMI research 2015;5:19. [PubMed: 25918673]

[32]. Zeglis BM, Sevak KK, Reiner T, Mohindra P, Carlin SD, Zanzonico P, et al. A pretargeted PET imaging strategy based on bioorthogonal Diels-Alder click chemistry. Journal of Nuclear Medicine 2013;54:1389–96. [PubMed: 23708196]

Author Manuscript Author Manuscript Author Manuscript Author Manuscript

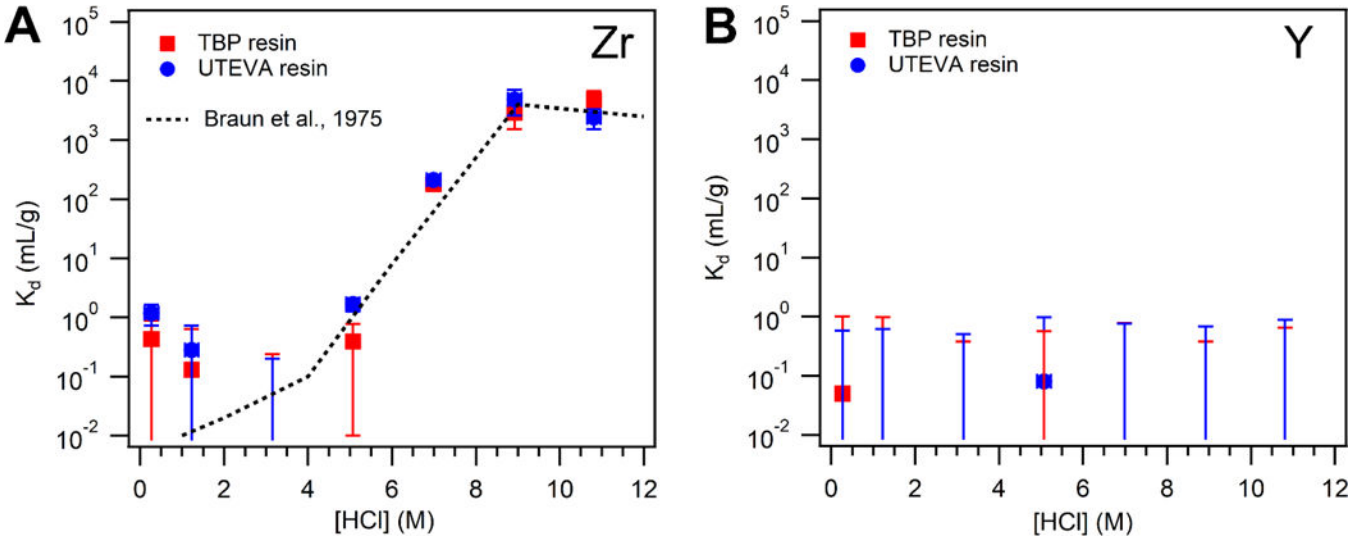

Figure 1.

Equilibrium coefficients for Zr (A) and Y (B) on TBP and UTEVA resin. Experiments were conducted with 1 mL of solution and ~110 mg of resin in each vial, agitated by a multi-tube vortexer for 24 hours prior to activity assay. Radioactivity concentration in the supernatant was subsequently quantified by filtering solids from an aliquot of the sample, followed by efficiency-calibrated HPGe gamma spectrometry.

Author Manuscript
Author Manuscript
Author Manuscript
Author Manuscript

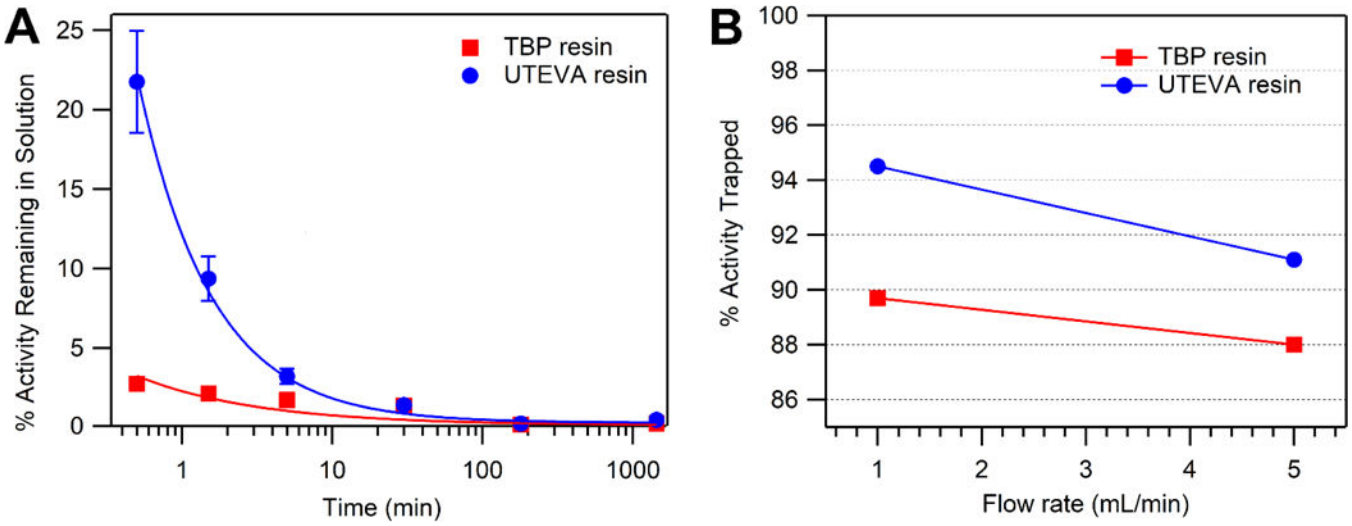

Figure 2.

(A) Reaction kinetics for binding of ^{89}Zr to TBP and UTEVA resins. TBP resin shows significantly faster binding kinetics compared with the UTEVA resin, with the percent activity remaining in solution dropping to less than 5% at <30 sec and 5 min respectively. (B) Column trapping as a function of flow-rate for TBP resin and UTEVA resin. Trend lines are eye-guides only.

Author Manuscript Author Manuscript Author Manuscript Author Manuscript

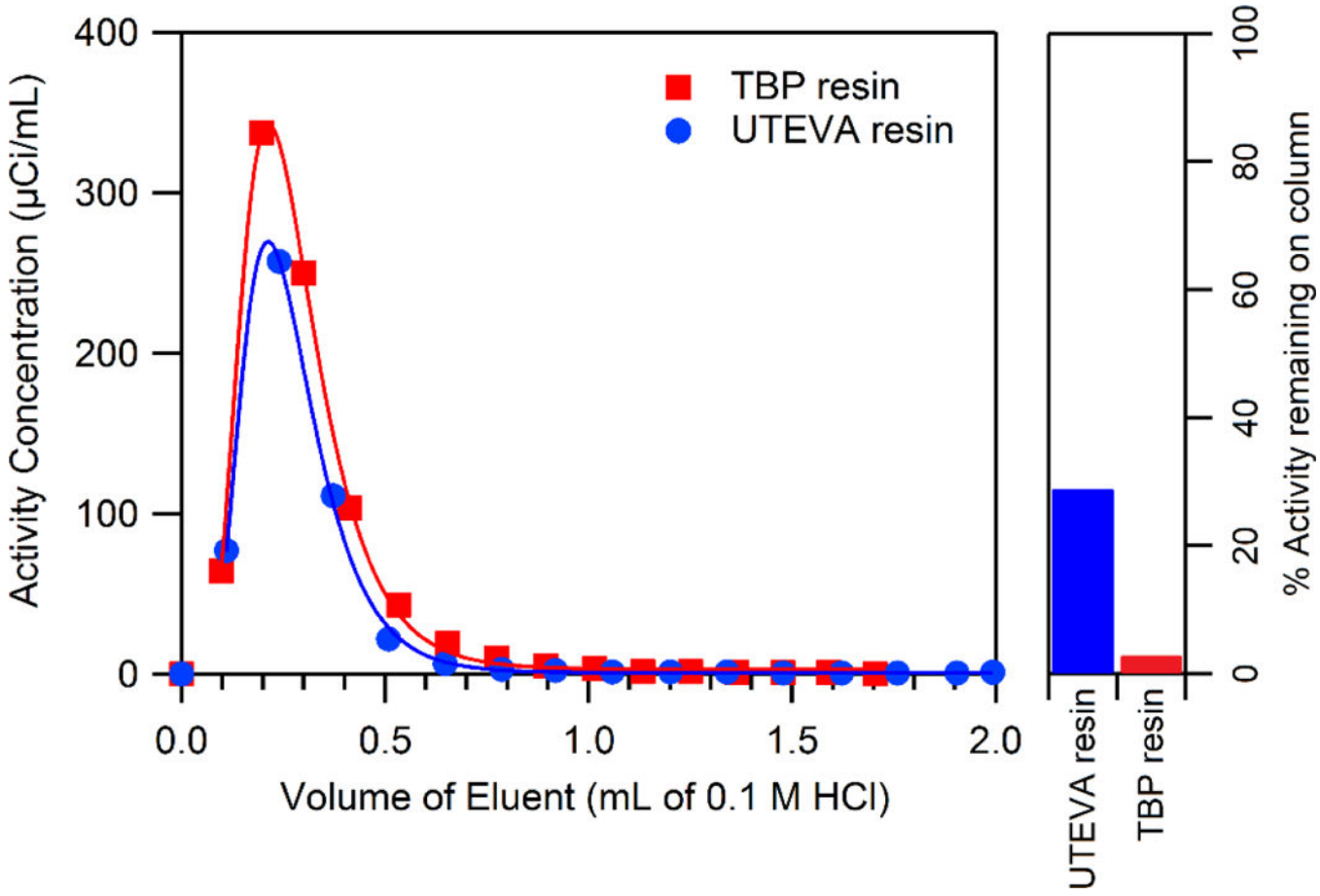

Figure 3.

Elution profiles of ^{89}Zr from 100 mg of TBP and UTEVA resin in 0.1 M HCl. The right bar-plot shows residual activity on each column, with the UTEVA column containing significantly more activity. This residual activity did not appear to behave chromatographically with further elution attempts with 0.1 M HCl, but the activity was readily removed from the column with 3 M HCl. Trend lines are eye-guides only.

Author Manuscript Author Manuscript Author Manuscript Author Manuscript

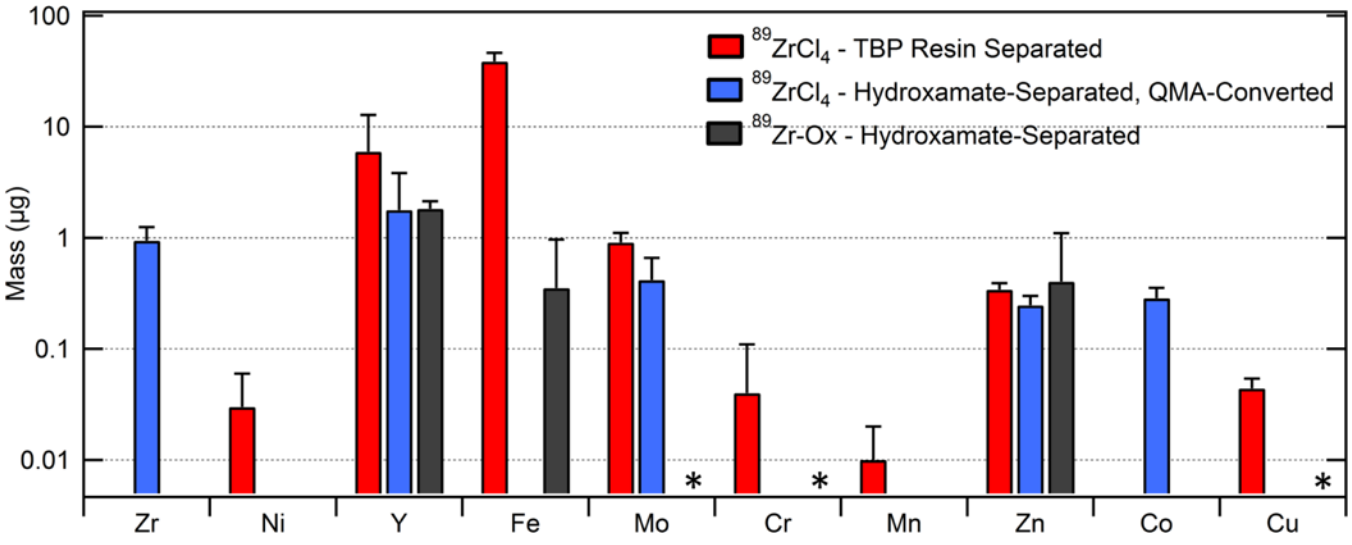

Figure 4.

Total trace metal impurities in ^{89}Zr products, as measured by MP-AES. Values represent mean ± standard deviation, corrected for the fraction of the total production activity tested. TBP resin-based isolations of ^{89}Zr-chloride (n = 3) and hydroxamate resin-based isolations of ^{89}Zr-oxalate (n = 3) were performed from full ^{nat}Y target masses. Samples converted from ^{89}Zr-chloride to ^{89}Zr-oxalate (n = 3) were obtained from an aliquot of a full production run. *Testing for Mo, Cr, and Cu was not available for ^{89}Zr-oxalate products.

Author Manuscript Author Manuscript Author Manuscript Author Manuscript

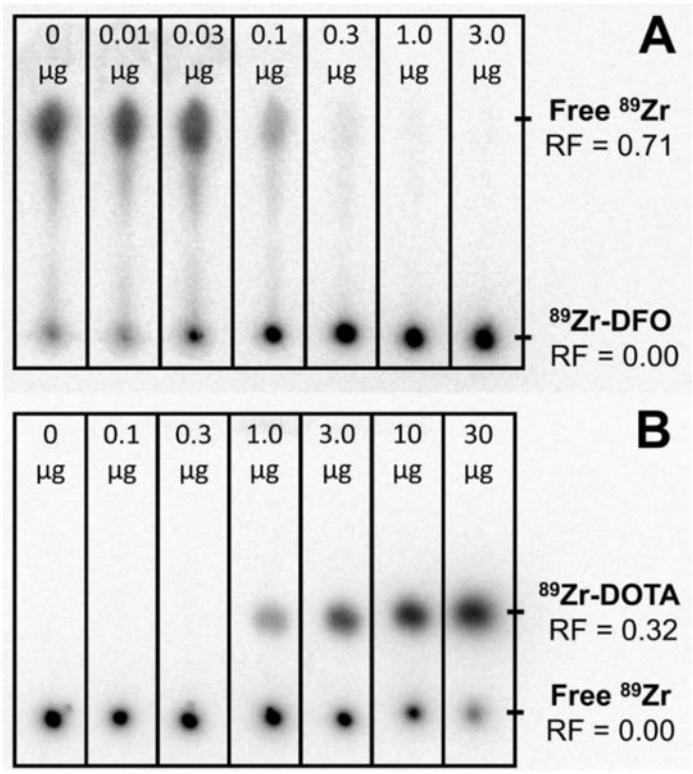

Figure 5.

Example radio-thin-layer chromatograph showing the separation of ^{89}Zr-DFO (A) and ^{89}Zr-DOTA (B) from unbound ^{89}Zr. Masses for each channel represent the mass of DFO or DOTA used for chelation per sample. For the separation of DFO-bound and unbound ^{89}Zr, DTPA was used to complex residual unbound ^{89}Zr.

Author Manuscript Author Manuscript Author Manuscript Author Manuscript

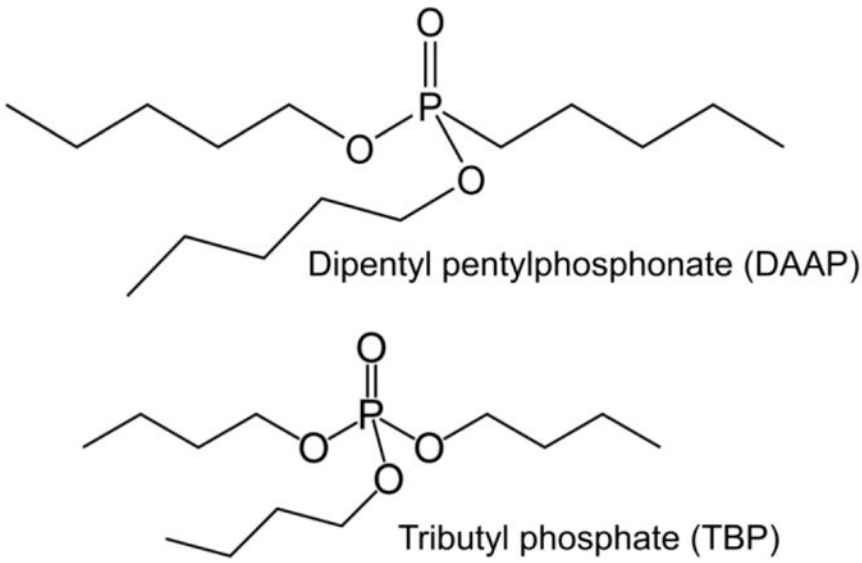

Figure 6.
Molecular structures of the dipentyl pentylphosphonate (DAAP) and tributyl phosphate (TBP) extractants.

Author Manuscript

Author Manuscript

Author Manuscript

Author Manuscript

Table 1.

Separation results for three TBP-based productions of ^{89}Zr-chloride. Residual ^{nat}Y mass was measured by microwave plasma atomic emission spectrometry (MP-AES).

Production	^{89}Zr Recovery	Initial ^{nat}Y mass	Residual ^{nat}Y mass	Separation Factor
1	90.4 %	395 mg	9.5 ± 1.0 μg	(3.8 ± 0.4) x10^4
2	85.4 %	355 mg	1.5 ± 0.3 μg	(1.9 ± 0.3) x10^5
3	91.9 %	434 mg	1.8 ± 0.2 μg	(2.2 ± 0.2) x10^5
Average	**89 ± 3 %**	**395 ± 40 mg**	**4.3 ± 4.5 μg**	**(1.5 ± 1.0) x10^5**